Supporting information

4-Cyanopyridine, a versatile mono- and bidentate ligand. Crystal structures of related coordination polymers determined by X-ray powder diffraction.

Haishuang Zhao,[a, b] Alexander Bodach,[a] Miriam Heine,[a] Yasar Krysiak,[a, b] Jürgen Glinnemann[a], Edith Alig[a] Lothar Fink,*[a] and Martin U. Schmidt[a]

[a] Institute of Inorganic and Analytical Chemistry, Goethe-University, Max-von-Laue-Str. 7, 60438 Frankfurt am Main, Germany. E-Mail: fink@chemie.uni-frankfurt.de; Fax: +49 69798 29235; Tel: +49 69798 29123

[b] Institute of Inorganic Chemistry and Analytical Chemistry, Johannes Gutenberg-University, Jakob-Welder-Weg 11, 55128 Mainz, Germany.

Figures

Fig. S1 DTA/TG curves of $[NiCl_2(4\text{-}CNpy)_2]_n$ (**3a**) 2
Fig. S2 DTA/TG curves of $[CoBr_2(4\text{-}CNpy)_2]_n$ (**4a**)..... 2
Fig. S3 DTA/TG curves of $[NiBr_2(4\text{-}CNpy)_2]_n$ (**5a**) 3
Fig. S4 Combined Rietveld refinement of $[CuCl_2(4\text{-}CNpy)]_n$ (**1b** sample **2**) 3
Fig. S5 Fragment of one layer in $[NiCl_2(4\text{-}CNpy)]_n$ (**3b**)..... 4
Fig. S6 IR spectrum of $[CuCl_2(4\text{-}CNpy)_2]_n$ (**1a**). 4
Fig. S7 Schematic representation for preparation of $[CuCl_2(4\text{-}CNpy)]_n$ (**1b**). 5
Fig. S8 IR spectrums of $[CuCl_2(4\text{-}CNpy)]_n$ (**1b**)..... 5
Fig. S9 IR spectrum of $[MnCl_2(4\text{-}CNpy)_2]_n$ (**2a**). 6
Fig. S10 IR spectrum of $[MnCl_2(4\text{-}CNpy)]_n$ (**2b**). 6
Fig. S11 IR spectrum of $[NiCl_2(4\text{-}CNpy)_2]_n$ (**3a**)..... 7
Fig. S12 IR spectrum of $[NiCl_2(4\text{-}CNpy)]_n$ (**3b**)..... 7
Fig. S13 IR spectrum of $[CoCl_2(4\text{-}CNpy)_2]_n$ (**4a**). 8
Fig. S 14 Schematic representation for preparation of $[CoBr_2(4\text{-}CNpy)]_n$ (**4b**)..... 8
Fig. S 15 IR spectrum of $[CoCl_2(4\text{-}CNpy)]_n$ (**4b**). 9
Fig. S16 IR spectrum of $[NiBr_2(4\text{-}CNpy)_2]_n$ (**5a**)..... 9
Fig. S17 IR spectrum of $[NiBr_2(4\text{-}CNpy)]_n$. (**5b**)..... 10
Fig. S18 Molecular structure model for structure solutions. 10

Tables

Table S1 Results of DTA/TG measurements. 11
Table S2 Results of quantitative Rietveld analysis for the three samples of $[CuCl_2(4\text{-}CNpy)]_n$ (**1b**). 11
Table S3 The mean bond lengths and bond angles in the given models in CSD.. 11

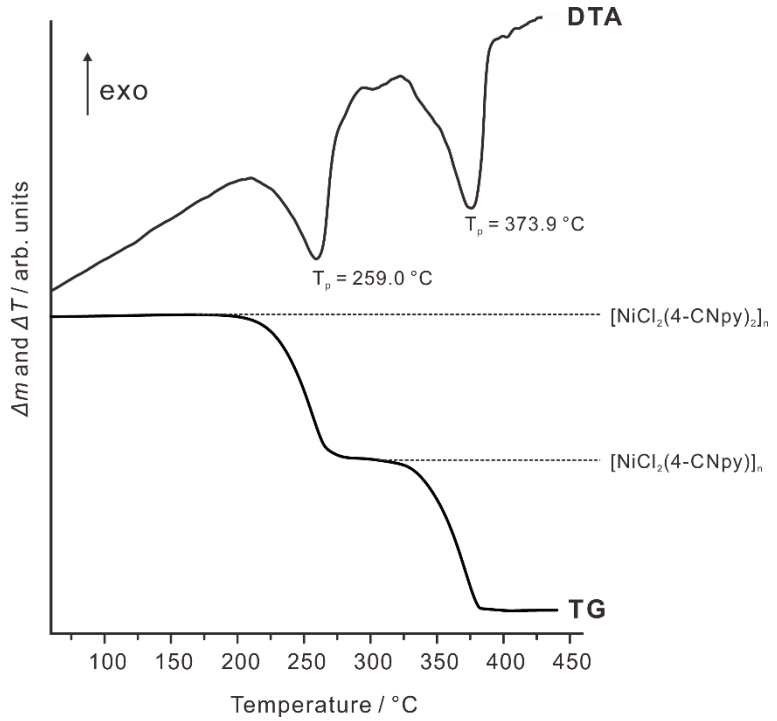

Fig. S1 DTA/TG curves of $[NiCl_2(4\text{-}CNpy)_2]_n$ (**3a**). Weight of starting compounds: 31.92 mg, Heating rate: 5 K/min, N_2 atmosphere, Al_2O_3 crucible, Tp: peak temperature.

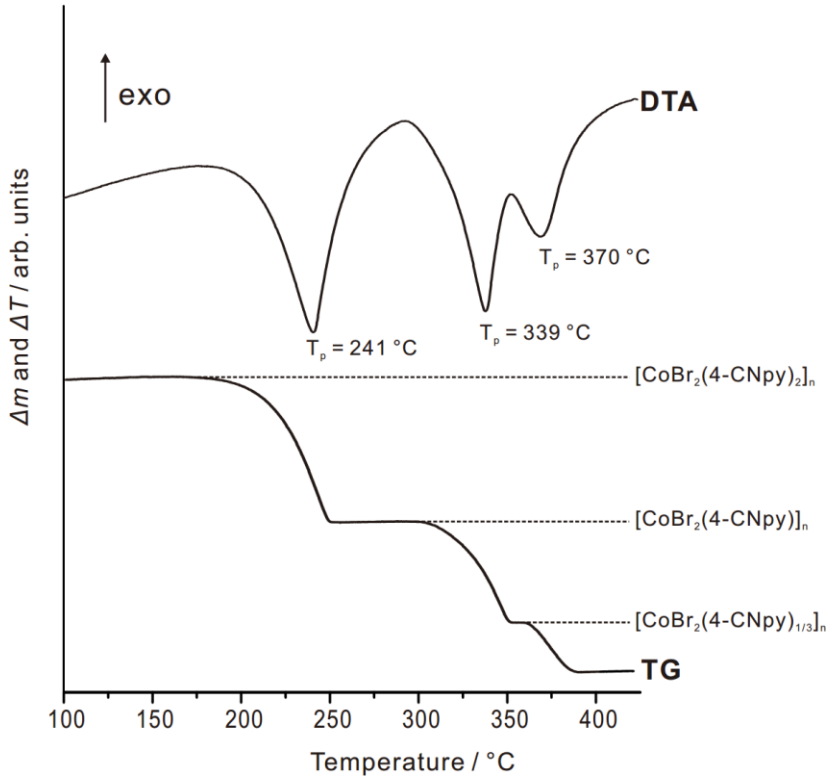

Fig. S2 DTA/TG curves of $[CoBr_2(4\text{-}CNpy)_2]_n$ (**4a**). Weight of starting compounds: 19.72 mg, Heating rate: 5 K/min, N_2 atmosphere, Al_2O_3 crucible, T_p: peak temperature.

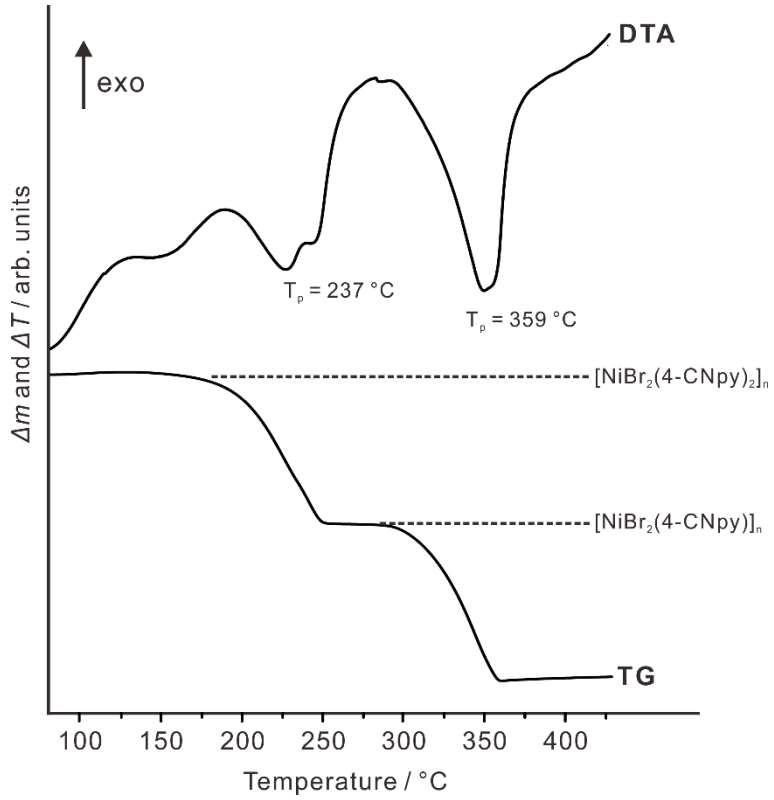

Fig. S3 DTA/TG curves of $[NiBr_2(4\text{-}CNpy)_2]_n$ (**5a**). Weight of starting compounds: 16.89 mg, Heating rate: 5 K/min, N_2 atmosphere, Al_2O_3 crucible, Tp: peak temperature.

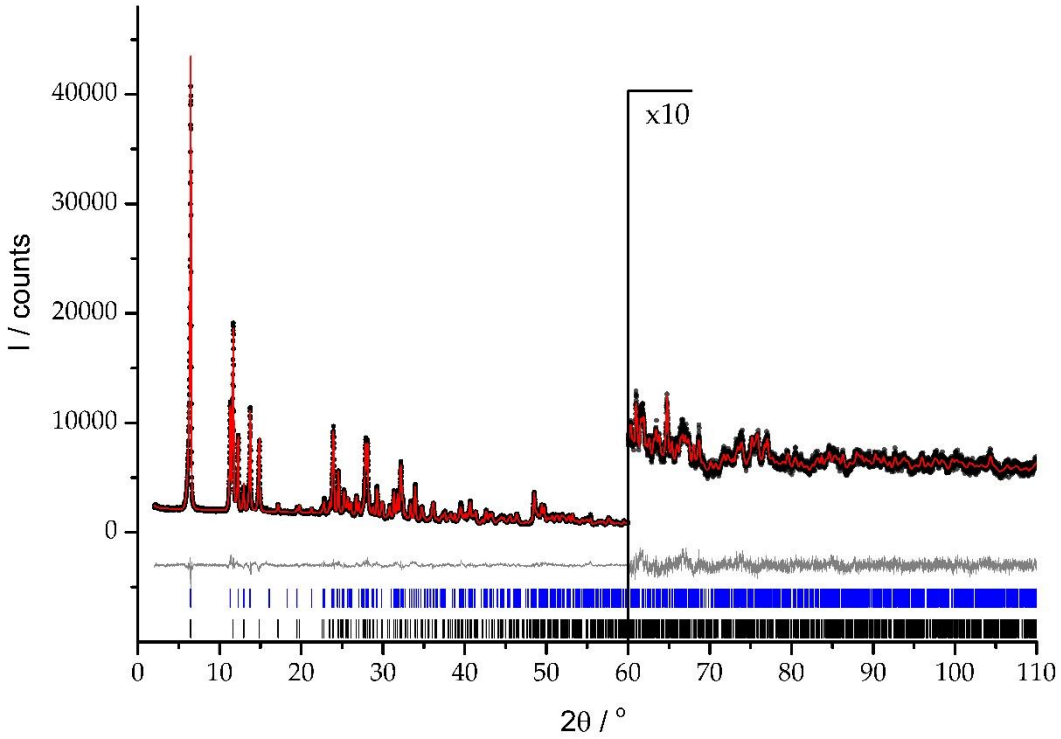

Fig. S4 Plot of combined Rietveld refinement of $[CuCl_2(4\text{-}CNpy)]_n$ **1b** (sample **2**). Observed powder diagram (black points), simulated powder diagram (red solid line), difference profiles (grey solid line), and reflection positions (blue (**α-1b** and black (**β-1b**) vertical lines). Change of the scale at 60º is with a factor of 10. Radiation type: Cu $K\alpha_1$ (λ= 1.54056 Å).

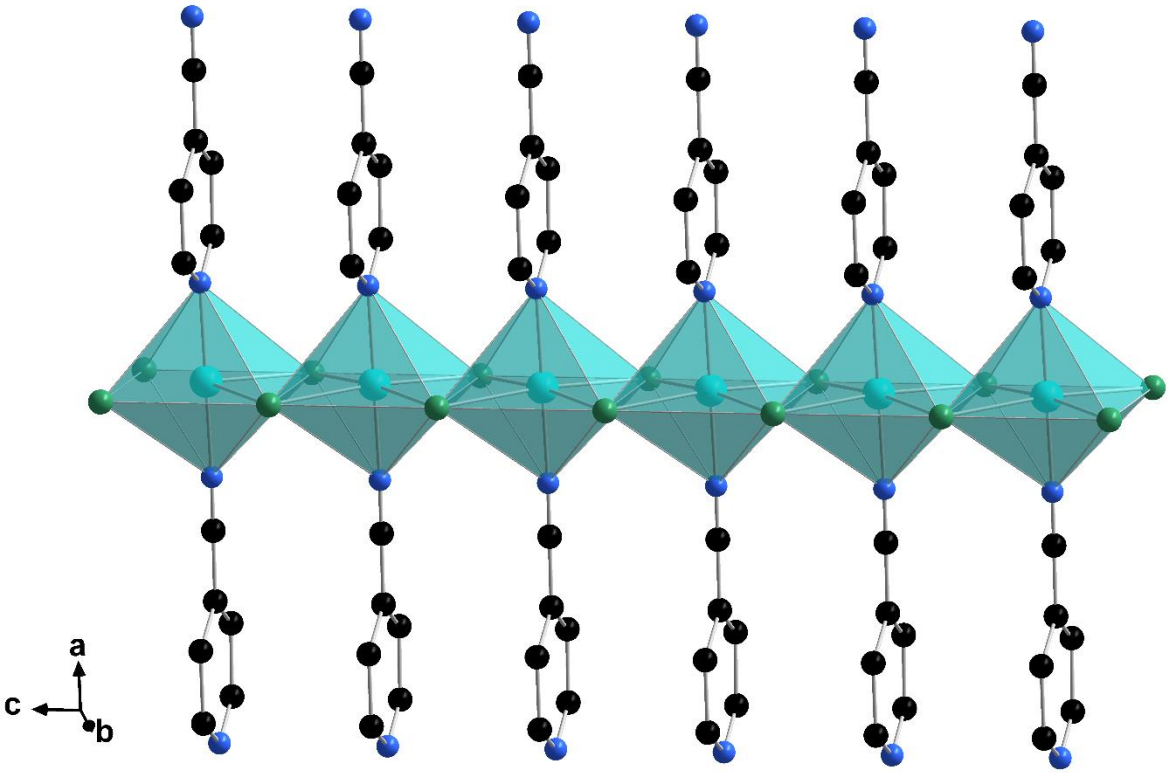

Fig. S5 Fragment of one layer in $[NiCl_2(4\text{-}CNpy)]_n$ (**3b**). H atoms have been removed for clarity.

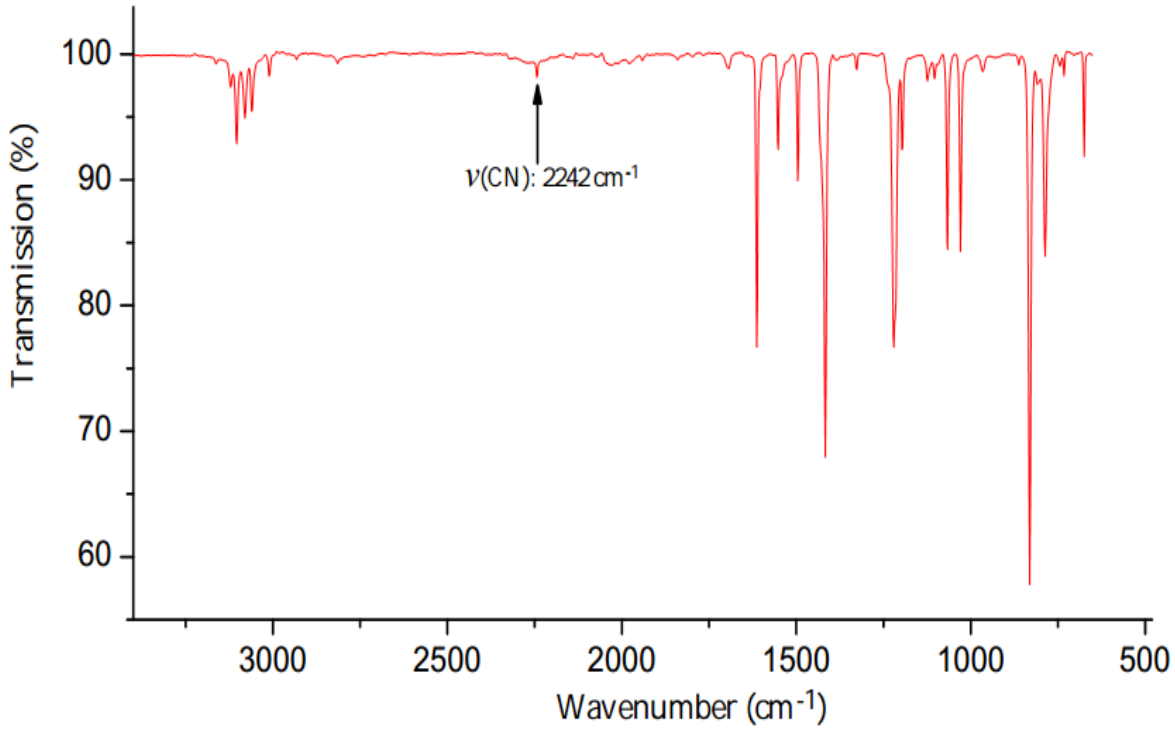

Fig. S6 IR spectrum of $[CuCl_2(4\text{-}CNpy)_2]_n$ (**1a**).

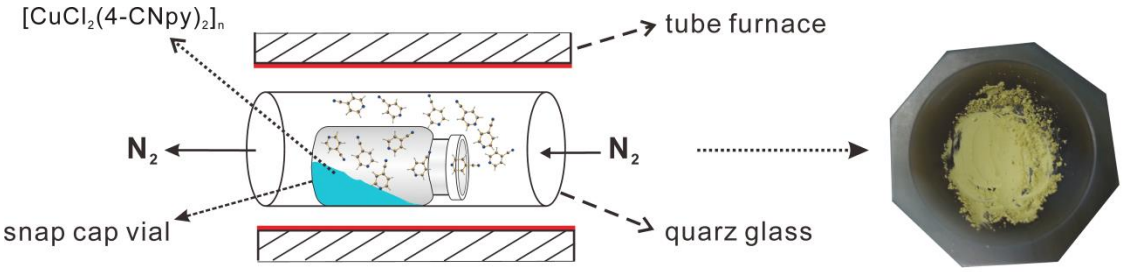

Fig. S7 Schematic representation for preparation of $[CuCl_2(4\text{-}CNpy)]_n$ (1b). According to the DTA/TG-curves of $[CuCl_2(4\text{-}CNpy)_2]_n$ (**1a**), the preparation of pure $[CuCl_2(4\text{-}CNpy)]_n$ (**1b**) was carried out using a snap cap vial as sample carrier under a controlled nitrogen flow.

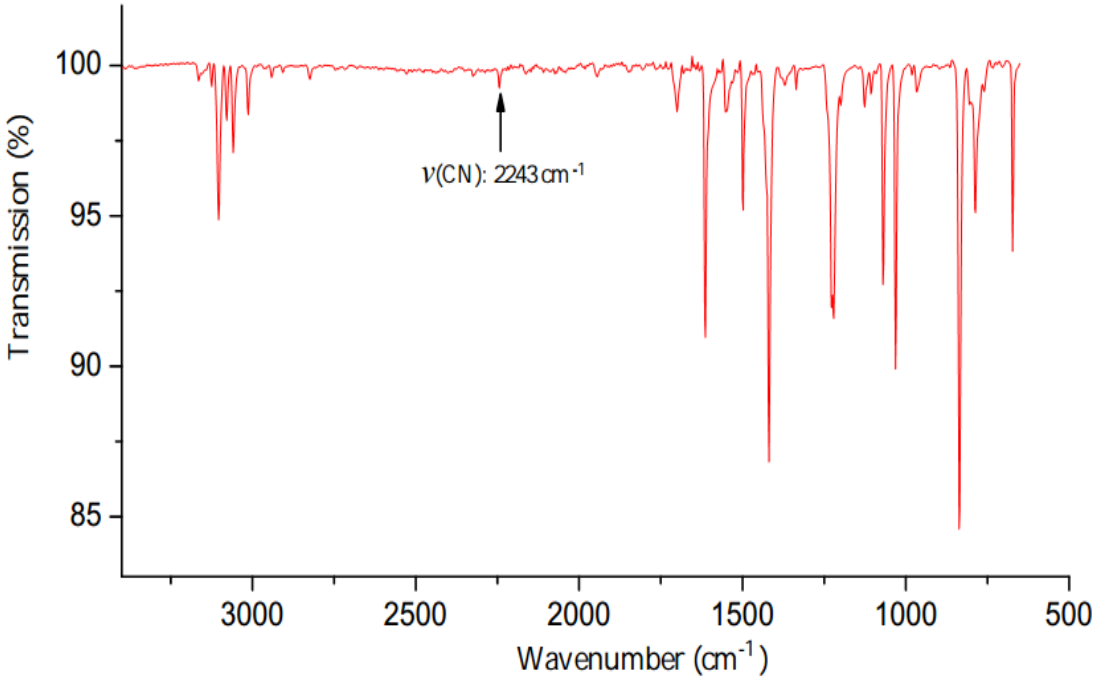

Fig. S8 IR spectrums of $[CuCl_2(4\text{-}CNpy)]_n$ **(1b)**.

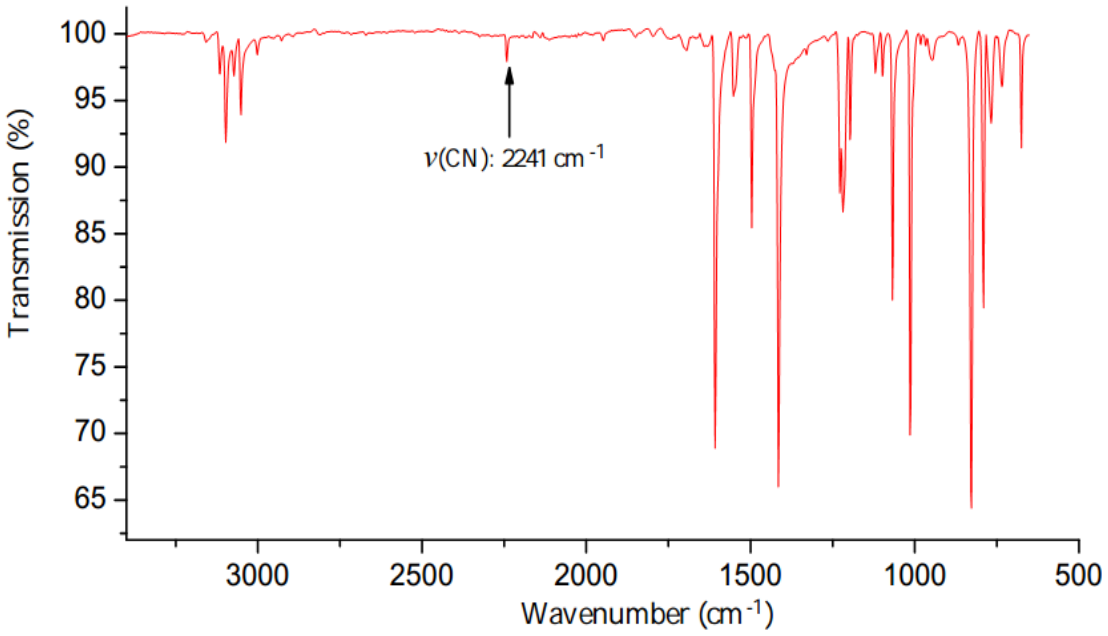

Fig. S9 IR spectrum of $[MnCl_2(4\text{-}CNpy)_2]_n$ **(2a)**.

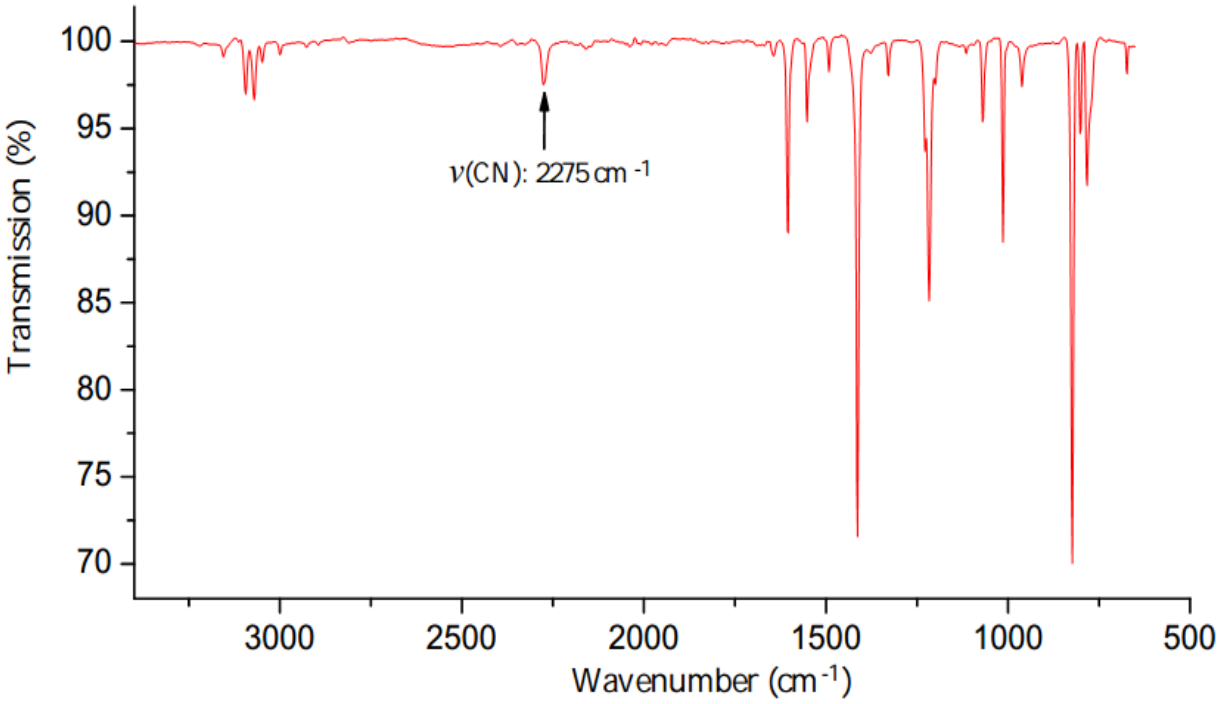

Fig. S10 IR spectrum of $[MnCl_2(4\text{-}CNpy)]_n$ **(2b)**.

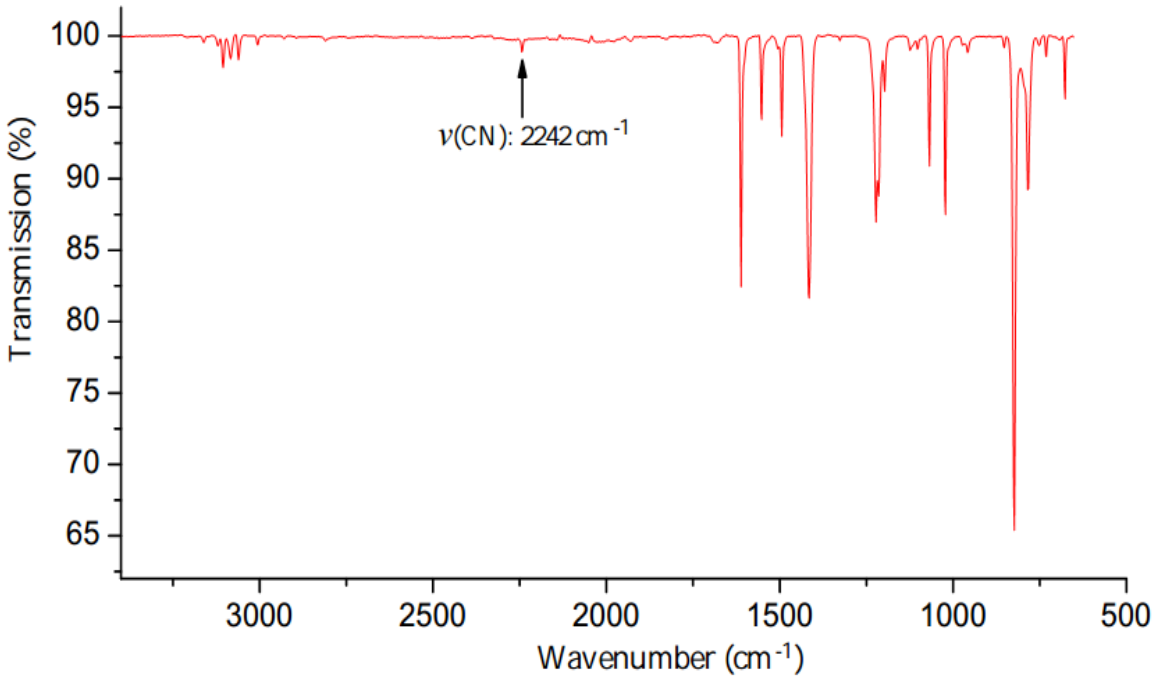

Fig. S11 IR spectrum of $[NiCl_2(4\text{-}CNpy)_2]_n$ **(3a)**.

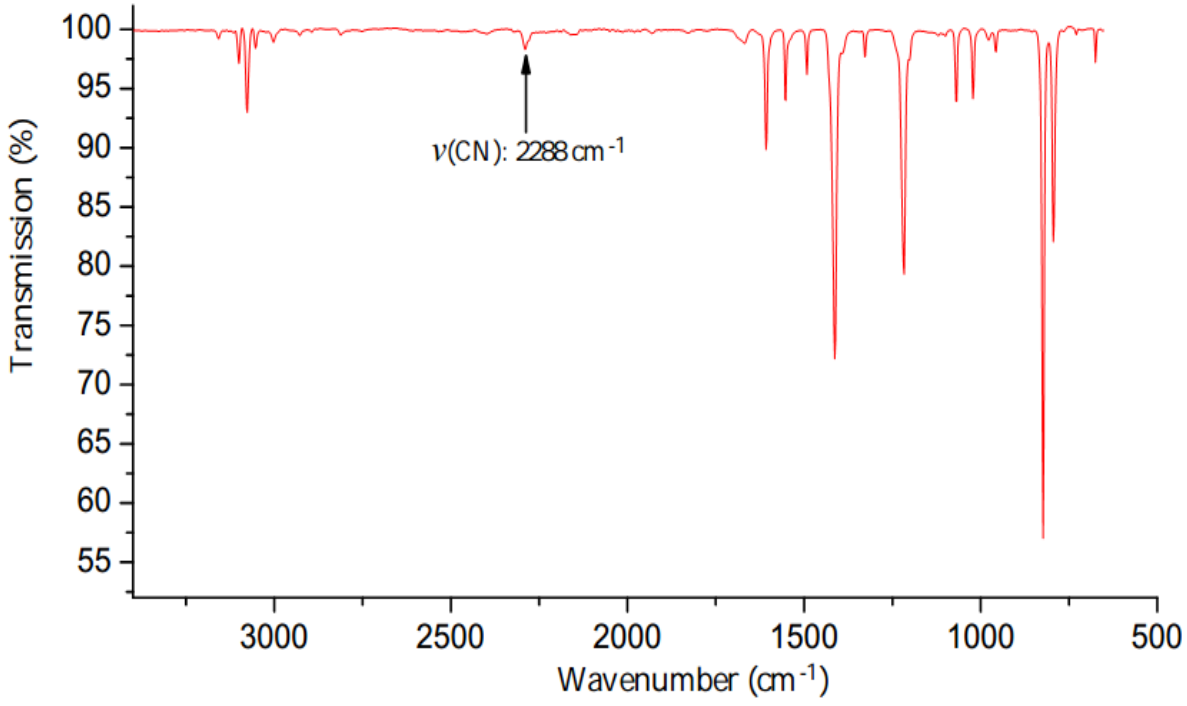

Fig. S12 IR spectrum of $[NiCl_2(4\text{-}CNpy)]_n$ **(3b)**.

.

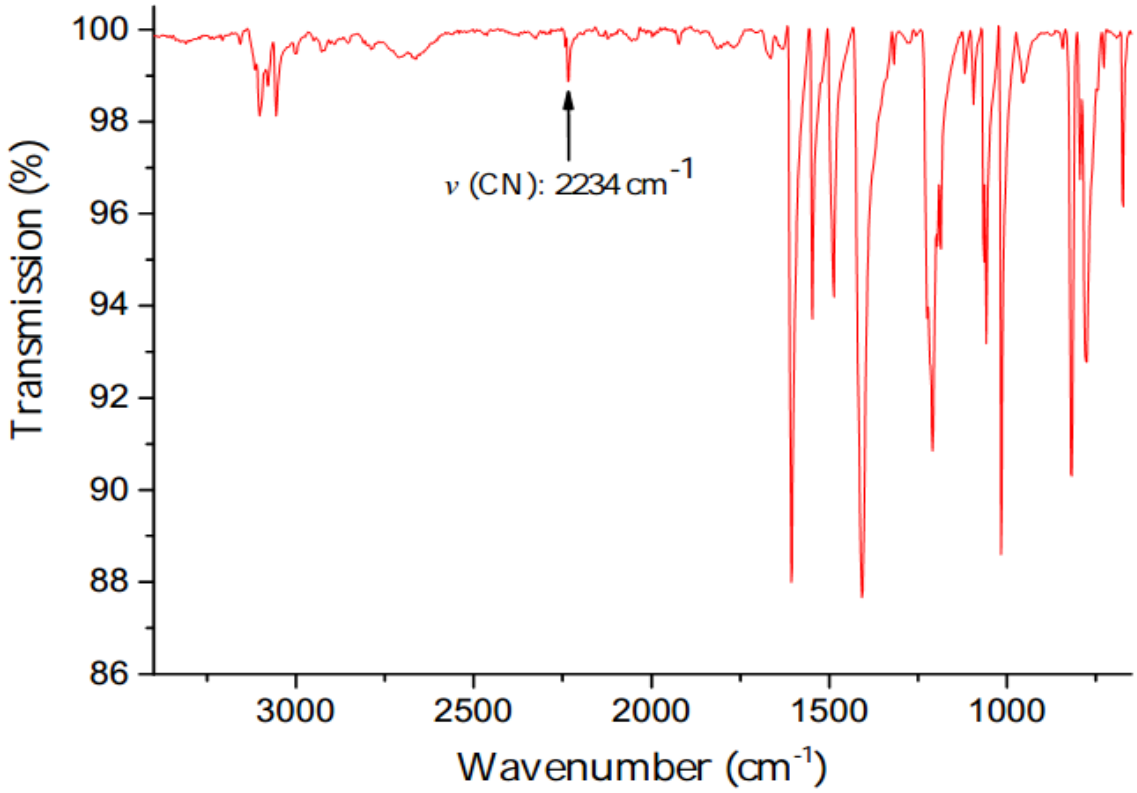

Fig. S13 IR spectrum of $[CoCl_2(4\text{-}CNpy)_2]_n$ **(4a)**.

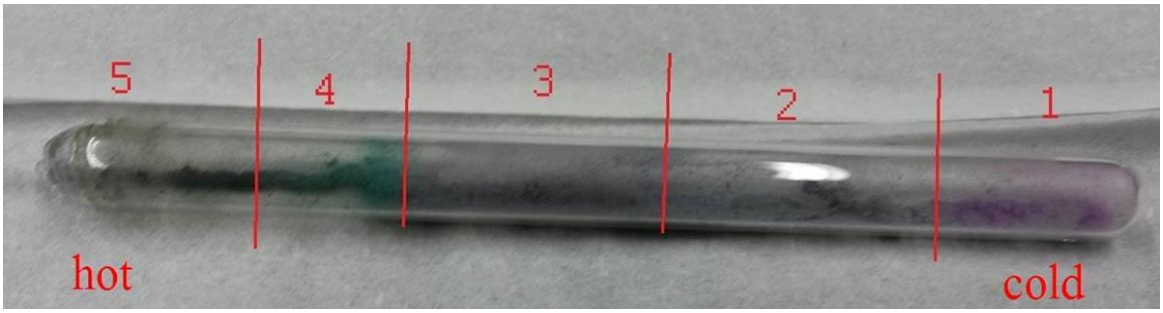

Fig. S 14 Schematic representation for preparation of $[CoBr_2(4\text{-}CNpy)]_n$ (**4b**).

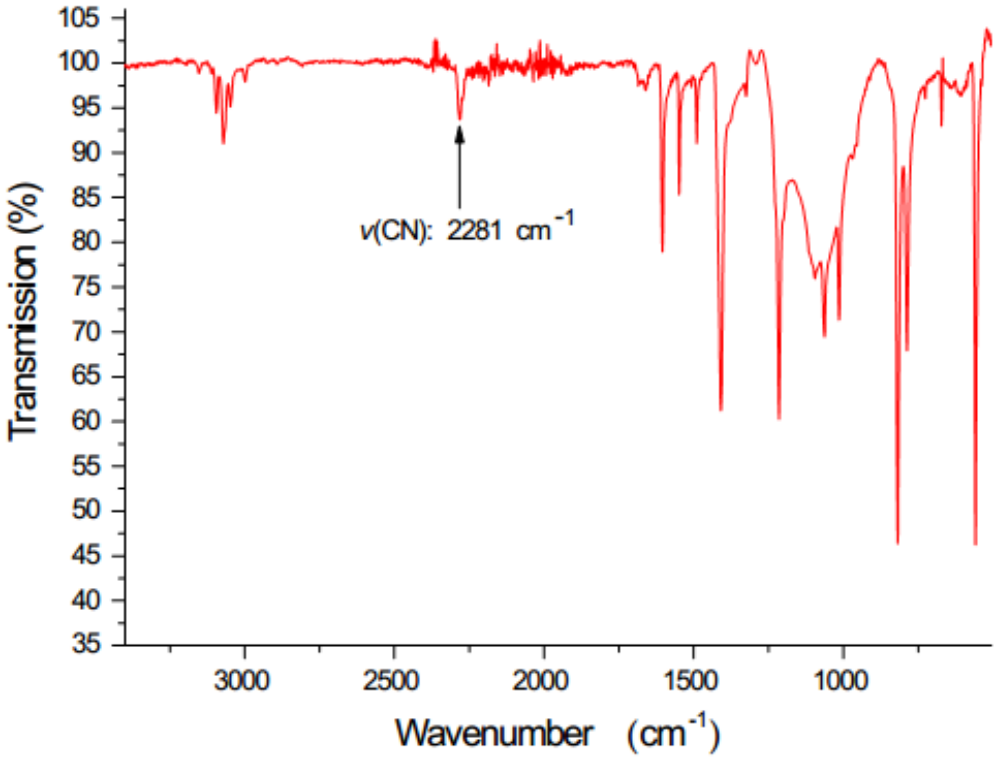

Fig. S 15 IR spectrum of $[CoCl_2(4\text{-}CNpy)]_n$ (**4b**).

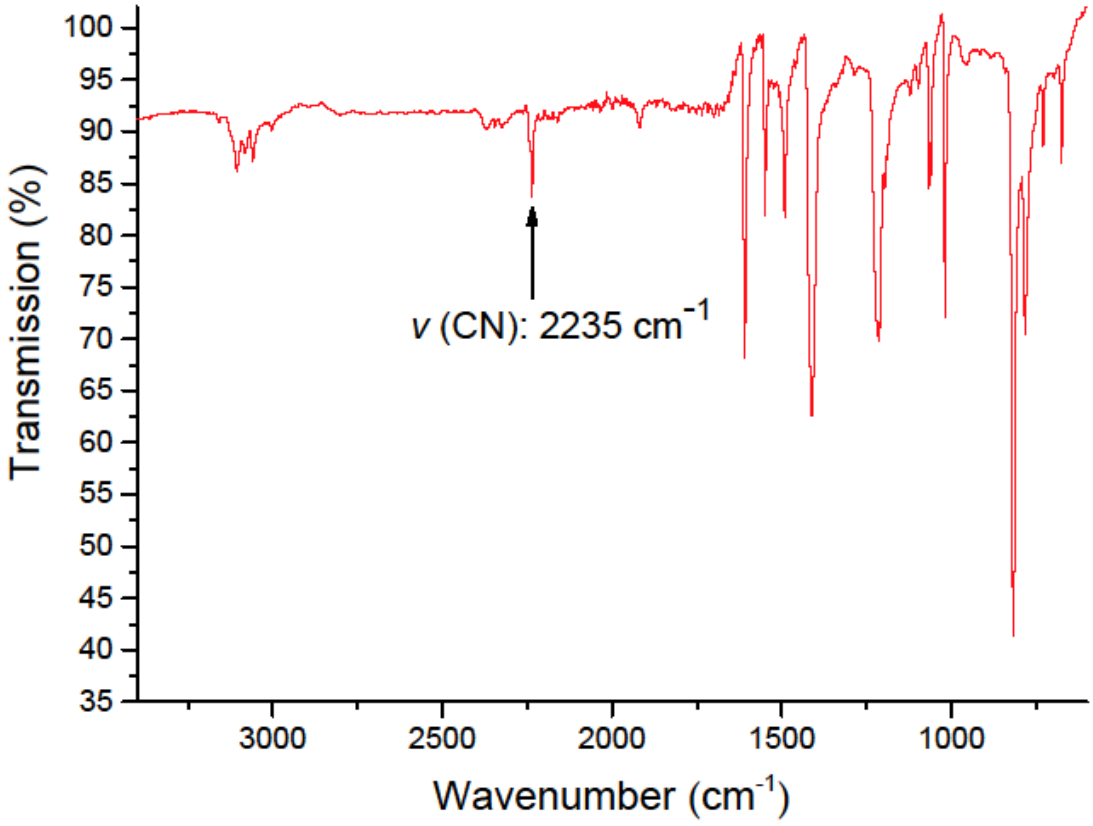

Fig. S16 IR spectrum of $[NiBr_2(4\text{-}CNpy)_2]_n$ **(5a)**.

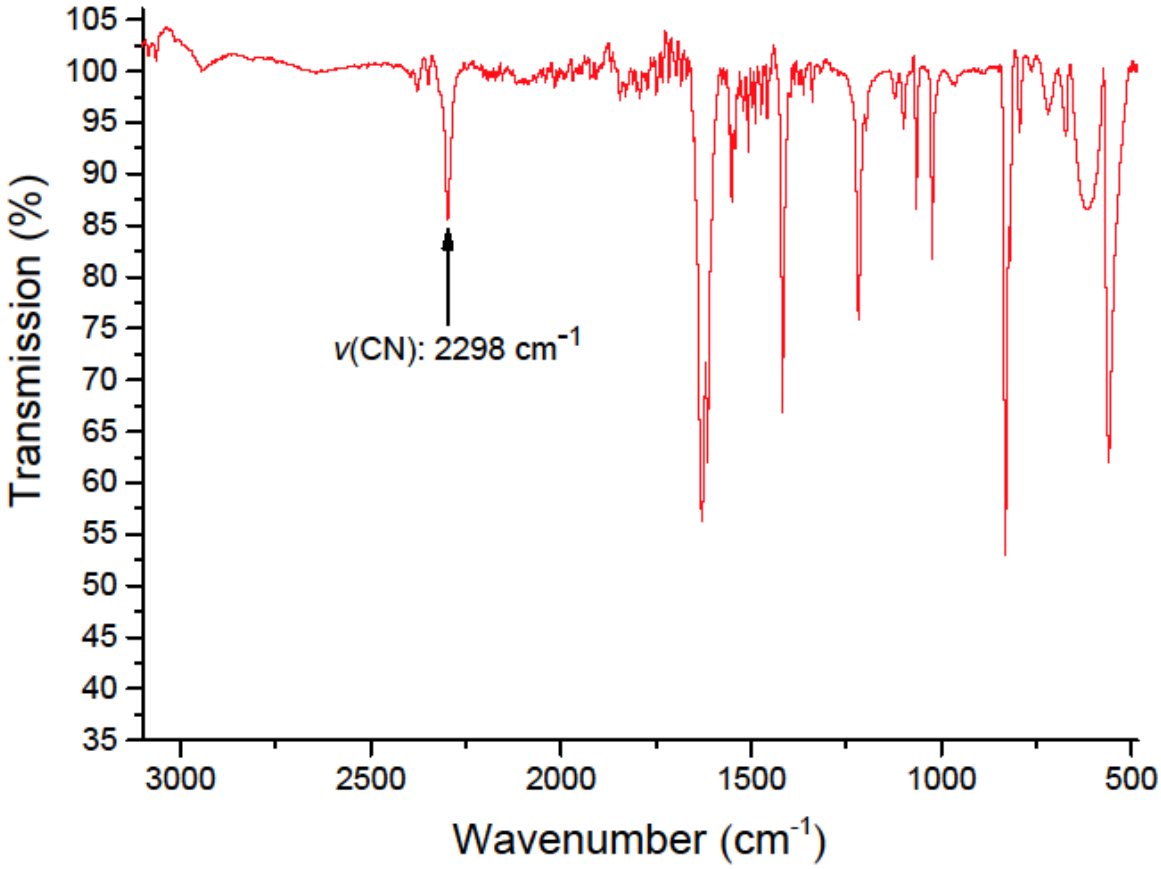

Fig. S17 IR spectrum of $[NiBr_2(4\text{-CNpy})]_n$. **(5b)**.

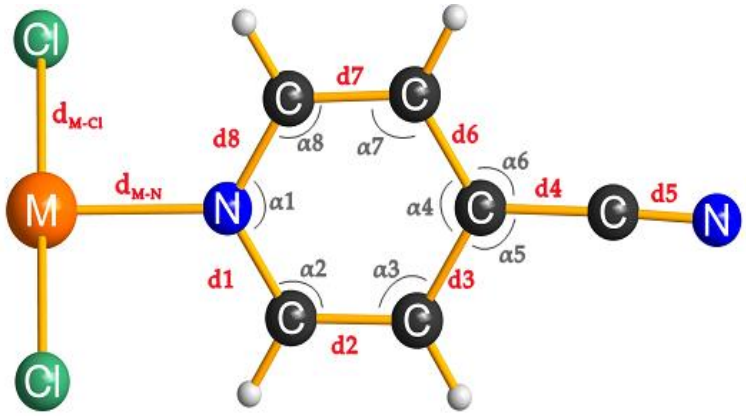

Fig. S18 Molecular structure model for structure solution. Note: model for compound **1b** - **4b**: MX_2(4-CNpy); for **3a** – **5a**: *MX*(4-CNpy) (*M* = Cu(II), Mn(II), Ni(II), Co(II), *X* = Cl, Br).

Table S1 Results of DTA/TG measurements of $[M(II)X_2(4\text{-}CNpy)_2]_n$ (M(II)= Cu, Mn, Ni, Co; X = Cl, Br). T: DTA peak temperatures, m_0: weight of starting compound, Δm_{exp}: relative experimental weight loss, experimental $\Delta m_{exp}/m_0$, calculated $\Delta m_{cal}/m_0$.

Compound	T /°C	m_0 /mg	Δm_{exp} /mg	$\Delta m_{exp}/m_0$ /%	$\Delta m_{cal}/m_0$ /%
$CuCl_2(4\text{-}CNpy)_2$	195	12.49	0	0	0
$CuCl_2(4\text{-}CNpy)$	267		3.63	29.1	30.38
$CuCl_2$	314		8.13	65.1	60.76
$MnCl_2(4\text{-}CNpy)_2$	190	17.18	0	0	0
$MnCl_2(4\text{-}CNpy)$	253		5.05	29.4	31.16
$MnCl_2(4\text{-}CNpy)_{1/3}$	318		8.54	49.7	51.94
$MnCl_2$	393		10.26	59.8	62.32
$NiCl_2(4\text{-}CNpy)_2$	200	31.92	0	0	0
$NiCl_2(4\text{-}CNpy)$	259		9.13	28.6	30.82
$NiCl_2$	374		18.79	58.9	61.63
$CoBr_2(4\text{-}CNpy)_2$	175	19.72	0	0	0
$CoBr_2(4\text{-}CNpy)$	241		4.51	22.9	24.38
$CoBr_2(4\text{-}CNpy)_{1/3}$	339		7.66	38.8	40.64
$CoBr_2$	370		9.20	46.7	48.77
$NiBr_2(4\text{-}CNpy)_2$	203	16.89	0	0	0
$NiBr_2(4\text{-}CNpy)$	325		3.81	22.58	24.37
$NiBr_2$	360		7.72	29.93	32.22

Table S2 Results of quantitative Rietveld analysis for the three samples of compound **1b**.

	α-1b /w%	**β-1b** /w%	R_{wp} /%	R_{exp} /%	*gof*
Sample **1**	72.76(18)	27.24(18)	4.41	2.53	1.74
Sample **2**	48.21(11)	51.79(11)	5.17	2.65	1.95
Sample **3**	14.87(20)	85.13(20)	5.89	2.82	2.09

Table S3 The mean bond lengths and bond angles in the given models after a statistic in CSD. $d1 = d8$, $d2 = d7$, $d3 = d6$; $a2 = a8$, $a3 = a7$, $a5 = a6$.

	1	**2**	**3**	**4**	**5**
bond angle ***a*** (º)	118.64	122.45	118.65	119.35	120.30
bond length ***d*** (Å)	1.338	1.377	1.381	1.447	1.138